PRAMANA © Indian Academy of Sciences Vol. 86, No. 6
— journal of June 2016
physics pp. 1343–1353

Analytical solutions of coupled-mode equations for microring resonators

C Y ZHAO[1,2]
[1]College of Science, Hangzhou Dianzi University, Zhejiang 310018, People's Republic of China
[2]State Key Laboratory of Quantum Optics and Quantum Optics Devices,
Institute of Opto-Electronics, Shanxi University, Taiyuan 030006, People's Republic of China
E-mail: zchy49@hdu.edu.cn

MS received 22 August 2014; revised 3 August 2015; accepted 7 September 2015
DOI: 10.1007/s12043-016-1200-3; ***e*Publication:** 7 April 2016

Abstract. We present a study on analytical solutions of coupled-mode equations for microring resonators with an emphasis on occurrence of all-optical EIT phenomenon, obtained by using a cofactor. As concrete examples, analytical solutions for a 3×3 linearly distributed coupler and a circularly distributed coupler are obtained. The former corresponds to a non-degenerate eigenvalue problem and the latter corresponds to a degenerate eigenvalue problem. For comparison and without loss of generality, analytical solution for a 4×4 linearly distributed coupler is also obtained. This paper may be of interest to optical physics and integrated photonics communities.

Keywords. Integrated optics; coupled resonators; analytical solutions; transmission.

PACS Nos 42.82.–m; 42.82.Et; 02.10.Yn

1. Introduction

As we know, in optical waveguide theory it is important to solve coupled-mode equations for optical fibre multiwaveguide systems. The coupled-mode theory is used to study the performance of single- and double-microring resonators [1–4]. Many atomic coherent effects can be realized using all-optical method, such as electromagnetic induction transparency (EIT), a multilevel atomic quantum interference phenomenon, and slow light, no inversion of laser, nonlinear optics and quantum information processing and so on. During the coupling-mode theoretical study of double microrings [5,6], we noticed that the interaction between double microring was ignored. Zheng *et al* first observed light EIT-like phenomenon in a controlled double microring coupling system [7]. Xiao *et al* realized the tunnelling-induced transparency effect in the chaotic optical microcavity [8]. The interaction between the microrings must be considered. Meng *et al* [9] evaluated coupled-mode equations for linearly distributed and circularly distributed multiwaveguide systems with the same coupled coefficients. We find that the 2×2 coupled system is equivalent to waveguide and single microring coupled system. The 3×3 coupled system is equivalent to waveguide and double microring coupled system. In this paper, we adopt a novel approach for obtaining coupled-mode equations for linearly distributed and circularly distributed multiwaveguide systems with different coupled coefficients. Furthermore, we investigate the transmission characteristics of asymmetric double microring coupled systems.

The cofactor is a very useful mathematical tool. To our knowledge, it is seldom applied in asymmetric double microrings analysis. In this paper, we adopt the cofactor to evaluate general solutions for asymmetric double microring systems in two kinds of coupling structures. The results obtained are compared with those of the previous studies to verify the method's effectiveness. The paper is organized as follows: Section 2 focusses on the 3×3 linearly distributed structure and 3×3 circularly distributed structure and the main conclusions are outlined. Section 3 focusses on the 4×4 linearly distributed structure. The main conclusions are outlined in §3.

2. The 3 × 3 asymmetric coupled resonators

As shown in figure 1, when the light circuits in counterclockwise direction in microring 2, we have $a_2 = B_2 b_2 = r_2 \mathrm{e}^{-j\theta} b_2$. When the light circuits in clockwise direction in microring 3, we have $a_3 = B_3 b_3 = r_3 \mathrm{e}^{j\theta} b_3$. Here, $\theta = \omega L/c$ is the phase shift. r_2, r_3 are the loss of microring 2, 3, respectively.

In this paper, we investigate how the coupling coefficient between optical fibres is different. $a_i(x_i)$ is the mode field in the ith waveguide, where $x_i = \beta/K$, $i = 1$–3, β is the mode propagation constant. $K/2$ denotes the coupling coefficient between adjacent waveguides. The coupling equation of the 3×3 asymmetric coupler is described in [9].

$$\begin{pmatrix} \dfrac{\partial a_1}{\partial z} \\ \dfrac{\partial a_2}{\partial z} \\ \dfrac{\partial a_3}{\partial z} \end{pmatrix} = \begin{pmatrix} 0 & j(K/2)\xi & j(K/2)\varsigma \\ j(K/2)\,\xi & 0 & j(K/2)\eta \\ j(K/2)\,\varsigma & j(K/2)\eta & 0 \end{pmatrix} \begin{pmatrix} a_1 \\ a_2 \\ a_3 \end{pmatrix}. \tag{1}$$

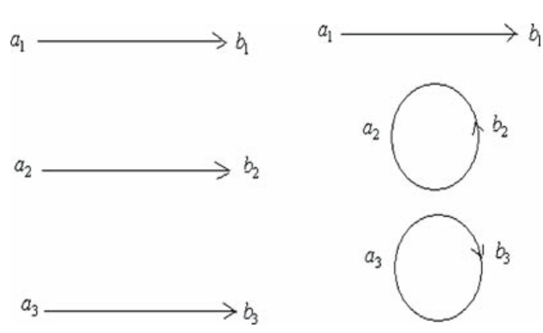

Figure 1. Schematic diagram of the 3×3 asymmetric coupler

We take $\lambda_i = -2x_i$, $i = 1$–3, the eigenfunction eq. (1) is

$$\begin{vmatrix} \lambda & \xi & \varsigma \\ \xi & \lambda & \eta \\ \varsigma & \eta & \lambda \end{vmatrix} = \lambda^3 - (\xi^2 + \eta^2 + \varsigma^2)\lambda + 2\xi\eta\varsigma = \lambda^3 + p\lambda + q = 0. \quad (2)$$

When $(p/3)^3 + (q/2)^2 < 0$, we assume $\lambda = n\cos[u]$, $u = \pi/3 + \varepsilon$, $n = \sqrt{-4p/3}$, and we have $\cos[3u] = 4\cos^3[u] - 3\cos[u] = -(q/2)(-p/3)^{-3/2}$. The eigenvalues λ_i are

$$\lambda_1 = n\cos[u] = n\chi_1, \qquad \lambda_2 = n\cos[u + 2\pi/3] = n\chi_2, \qquad \lambda_3 = n\cos[u + 4\pi/3] = n\chi_3,$$

where

$$\chi_1 = x = \cos[u], \qquad \chi_2 = -\frac{1}{2}x - \frac{\sqrt{3}}{2}\sqrt{1-x^2}, \qquad \chi_3 = -\frac{1}{2}x + \frac{\sqrt{3}}{2}\sqrt{1-x^2}. \quad (3)$$

Setting $\partial a_i/\partial z = -\lambda a_i$, $i = 1$–3, we have $a_i(x_m) = \varphi_i(\chi_m)\mathrm{e}^{j\beta z} = \varphi_i(\chi_m)\mathrm{e}^{jx_m\tau}$. If the eigenvalue χ_i is given, the corresponding eigenvector $\varphi_i(\chi_i)$, $i = 1$–3 can be given out by the cofactor A_{ij}, $i, j = 1$–3 (see Appendix A).

$$\varphi_1(\chi_i) = \frac{n^2\chi_i^2 - \eta^2}{N_i}, \quad \varphi_2(\chi_i) = \frac{\eta\varsigma - n\xi\chi_i}{N_i}, \quad \varphi_3(\chi_i) = \frac{\xi\eta - n\varsigma\chi_i}{N_i},$$

$$N_i = \sqrt{(\eta\varsigma - n\xi\chi_i)^2 + (\xi\eta - n\varsigma\chi_i)^2 + (n^2\chi_i^2 - \eta^2)^2}, \quad i = 1\text{–}3 \quad (4)$$

and satisfy the orthogonal relation $\varphi_1(\chi_1)\varphi_1(\chi_2) + \varphi_2(\chi_1)\varphi_2(\chi_2) + \varphi_3(\chi_1)\varphi_3(\chi_2) = 0$. As the eigenvalues χ_i are different from one another, we can use the eigensolution $a_i(x_i)$ to construct a solution matrix

$$\chi(\tau) = \begin{pmatrix} \varphi_1(\chi_1)\mathrm{e}^{ix_1\tau} & \varphi_1(\chi_2)\mathrm{e}^{ix_2\tau} & \varphi_1(\chi_3)\mathrm{e}^{ix_3\tau} \\ \varphi_2(\chi_1)\mathrm{e}^{ix_1\tau} & \varphi_2(\chi_2)\mathrm{e}^{ix_2\tau} & \varphi_2(\chi_3)\mathrm{e}^{ix_3\tau} \\ \varphi_3(\chi_1)\mathrm{e}^{ix_1\tau} & \varphi_3(\chi_2)\mathrm{e}^{ix_2\tau} & \varphi_3(\chi_3)\mathrm{e}^{ix_3\tau} \end{pmatrix}, \quad (5)$$

When $\tau \to 0$, corresponding to the starting point of the coupling zone,

$$\chi^{-1}(0) = \begin{pmatrix} \tilde{\varphi}_1(\chi_1) & \tilde{\varphi}_2(\chi_1) & \tilde{\varphi}_3(\chi_1) \\ \tilde{\varphi}_1(\chi_2) & \tilde{\varphi}_2(\chi_2) & \tilde{\varphi}_3(\chi_2) \\ \tilde{\varphi}_1(\chi_3) & \tilde{\varphi}_2(\chi_3) & \tilde{\varphi}_3(\chi_3) \end{pmatrix}, \quad (6)$$

where

$$\tilde{\varphi}_3(\chi_2) = \frac{(n^2\varsigma\eta\chi_2 + n^3\xi\chi_1\chi_3 + n\eta^2\xi)(\chi_1 - \chi_3)}{N_1 N_3 \Delta},$$

$$\tilde{\varphi}_3(\chi_3) = \frac{(n^2\varsigma\eta\chi_3 + n^3\xi\chi_1\chi_2 + n\eta^2\xi)(\chi_2 - \chi_1)}{N_1 N_2 \Delta},$$

$$\Delta = \begin{vmatrix} \varphi_1(\chi_1) & \varphi_1(\chi_2) & \varphi_1(\chi_3) \\ \varphi_2(\chi_1) & \varphi_2(\chi_2) & \varphi_2(\chi_3) \\ \varphi_3(\chi_1) & \varphi_3(\chi_2) & \varphi_3(\chi_3) \end{vmatrix},$$

$$\tilde{\varphi}_1(\chi_1) = \frac{n\eta(\xi^2 - \varsigma^2)(\chi_3 - \chi_2)}{N_2 N_3 \Delta},$$

$$\tilde{\varphi}_2(\chi_1) = \frac{(n^2\xi\eta\chi_1 + n^3\varsigma\chi_2\chi_3 + n\eta^2\varsigma)(\chi_2 - \chi_3)}{N_2N_3\Delta},$$
$$\tilde{\varphi}_1(\chi_2) = \frac{n\eta(\xi^2 - \varsigma^2)(\chi_1 - \chi_3)}{N_1N_3\Delta},$$
$$\tilde{\varphi}_2(\chi_2) = \frac{(n^2\xi\eta\chi_2 + n^3\varsigma\chi_1\chi_3 + n\eta^2\varsigma)(\chi_3 - \chi_1)}{N_1N_3\Delta},$$
$$\tilde{\varphi}_1(\chi_3) = \frac{n\eta(\xi^2 - \varsigma^2)(\chi_2 - \chi_1)}{N_1N_2\Delta},$$
$$\tilde{\varphi}_2(\chi_3) = \frac{(n^2\xi\eta\chi_3 + n^3\varsigma\chi_1\chi_2 + n\eta^2\varsigma)(\chi_1 - \chi_2)}{N_1N_2\Delta}.$$
$$\tilde{\varphi}_3(\chi_1) = \frac{(n^2\varsigma\eta\chi_1 + n^3\xi\chi_2\chi_3 + n\eta^2\xi)(\chi_3 - \chi_2)}{N_2N_3\Delta}. \quad (7)$$

The transform matrix

$$R(\tau) = \chi(\tau)\chi^{-1}(0) = \begin{pmatrix} \alpha_1 & \delta & \mu \\ \kappa & \alpha_2 & \rho \\ \nu & \zeta & \alpha_3 \end{pmatrix},$$

where

$$\alpha_1 = \varphi_1(\chi_1)\tilde{\varphi}_1(\chi_1)\,\mathrm{e}^{jx_1\tau} + \varphi_1(\chi_2)\tilde{\varphi}_1(\chi_2)\mathrm{e}^{jx_2\tau} + \varphi_1(\chi_3)\tilde{\varphi}_1(\chi_3)\mathrm{e}^{jx_3\tau},$$
$$\kappa = \varphi_2(\chi_1)\tilde{\varphi}_1(\chi_1)\,\mathrm{e}^{jx_1\tau} + \varphi_2(\chi_2)\tilde{\varphi}_1(\chi_2)\mathrm{e}^{jx_2\tau} + \varphi_2(\chi_3)\tilde{\varphi}_1(\chi_3)\mathrm{e}^{jx_3\tau},$$
$$\nu = \varphi_3(\chi_1)\tilde{\varphi}_1(\chi_1)\,\mathrm{e}^{jx_1\tau} + \varphi_3(\chi_2)\tilde{\varphi}_1(\chi_2)\mathrm{e}^{jx_2\tau} + \varphi_3(\chi_3)\tilde{\varphi}_1(\chi_3)\mathrm{e}^{jx_3\tau},$$
$$\delta = \varphi_1(\chi_1)\tilde{\varphi}_2(\chi_1)\,\mathrm{e}^{jx_1\tau} + \varphi_1(\chi_2)\tilde{\varphi}_2(\chi_2)\mathrm{e}^{jx_2\tau} + \varphi_1(\chi_3)\tilde{\varphi}_2(\chi_3)\mathrm{e}^{jx_3\tau},$$
$$\alpha_2 = \varphi_2(\chi_1)\tilde{\varphi}_2(\chi_1)\,\mathrm{e}^{jx_1\tau} + \varphi_2(\chi_2)\tilde{\varphi}_2(\chi_2)\mathrm{e}^{jx_2\tau} + \varphi_2(\chi_3)\tilde{\varphi}_2(\chi_3)\mathrm{e}^{jx_3\tau},$$
$$\zeta = \varphi_3(\chi_1)\tilde{\varphi}_2(\chi_1)\,\mathrm{e}^{jx_1\tau} + \varphi_3(\chi_2)\tilde{\varphi}_2(\chi_2)\mathrm{e}^{jx_2\tau} + \varphi_3(\chi_3)\tilde{\varphi}_2(\chi_3)\mathrm{e}^{jx_3\tau},$$
$$\mu = \varphi_1(\chi_1)\tilde{\varphi}_3(\chi_1)\,\mathrm{e}^{jx_1\tau} + \varphi_1(\chi_2)\tilde{\varphi}_3(\chi_2)\mathrm{e}^{jx_2\tau} + \varphi_1(\chi_3)\tilde{\varphi}_3(\chi_3)\mathrm{e}^{jx_3\tau},$$
$$\rho = \varphi_2(\chi_1)\tilde{\varphi}_3(\chi_1)\,\mathrm{e}^{jx_1\tau} + \varphi_2(\chi_2)\tilde{\varphi}_3(\chi_2)\mathrm{e}^{jx_2\tau} + \varphi_2(\chi_3)\tilde{\varphi}_3(\chi_3)\mathrm{e}^{jx_3\tau},$$
$$\alpha_3 = \varphi_3(\chi_1)\tilde{\varphi}_3(\chi_1)\,\mathrm{e}^{jx_1\tau} + \varphi_3(\chi_2)\tilde{\varphi}_3(\chi_2)\mathrm{e}^{jx_2\tau} + \varphi_3(\chi_3)\tilde{\varphi}_3(\chi_3)\mathrm{e}^{jx_3\tau}. \quad (8)$$

The output field (b_1, b_2, b_3) is related to the input field (a_1, a_2, a_3) by the transform matrix form

$$\begin{pmatrix} b_1 \\ b_2 \\ b_3 \end{pmatrix} = R(\tau)\begin{pmatrix} a_1 \\ a_2 \\ a_3 \end{pmatrix} = \begin{pmatrix} \alpha_1 & \delta & \mu \\ \kappa & \alpha_2 & \rho \\ \nu & \zeta & \alpha_3 \end{pmatrix}\begin{pmatrix} a_1 \\ B_2b_2 \\ B_3b_3 \end{pmatrix}. \quad (9)$$

We can easily find that the 3×3 coupler is equivalent to the coupled double-ring resonator.

2.1 *Linearly distributed*

Setting $\xi = 1$, $\eta = 1$, $\varsigma = 0$ and $\xi^2 + \eta^2 = 2$, we have $p = -2$, $q = 0$, $n = 2\sqrt{2}/\sqrt{3}$. Substituting it into eq. (3), the eigenvalues are

$$x_1 = 0, \quad x_2 = 1/\sqrt{2}, \quad x_3 = -1/\sqrt{2} \tag{10}$$

and the transform matrix

$$R(\tau) = \begin{pmatrix} (1/\sqrt{2})\mathrm{e}^{ix_1\tau} & (1/2)\mathrm{e}^{jx_2\tau} & (1/2)\mathrm{e}^{jx_3\tau} \\ 0 & (1/\sqrt{2})\mathrm{e}^{jx_2\tau} & -(1/\sqrt{2})\mathrm{e}^{jx_3\tau} \\ -(1/\sqrt{2})\mathrm{e}^{ix_1\tau} & (1/2)\mathrm{e}^{jx_2\tau} & (1/2)\mathrm{e}^{jx_3\tau} \end{pmatrix} \times \begin{pmatrix} 1/\sqrt{2} & 0 & -1/\sqrt{2} \\ 1/2 & 1/\sqrt{2} & 1/2 \\ 1/2 & -1/\sqrt{2} & 1/2 \end{pmatrix}. \tag{11}$$

Equation (11) is the same as eq. (22) in ref. [9]. Here $t = \cos[\tau/\sqrt{2}]$.

Eliminating b_1, b_3 from eq. (9), the transmission assumes a simplified form

$$T = \left| \frac{\alpha_1 - \alpha_3 B_2 - \alpha_2 B_3 + B_2 B_3}{1 - \alpha_2 B_2 \quad - \alpha_3 B_3 + \alpha_1 B_2 B_3} \right|^2. \tag{12}$$

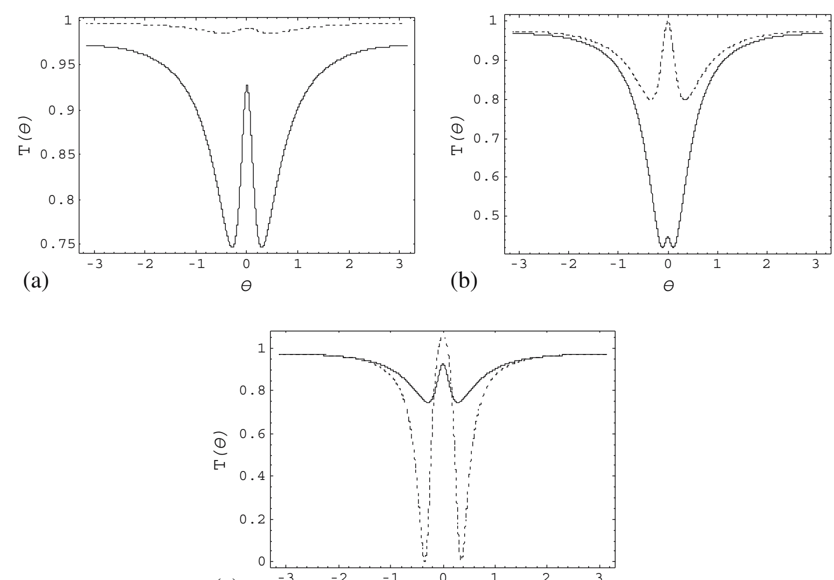

Figure 2. The transmission spectrum of double microring coupled system. For example we take $\alpha_1 = r_2 r_3$, $\alpha_3 = \alpha_2 + 1 - \alpha_1$. (**a**) $t = 0.80$, $r_3 = 0.99$, $r_2 = 0.85$ (solid line), $r_2 = 0.95$ (dashed line), (**b**) $t = 0.80$, $r_2 = 0.85$, $r_3 = 0.96$ (solid line), $r_3 = 1.0$ (dashed line), (**c**) $r_2 = 0.85$, $r_3 = 0.99$, $t = 0.80$ (solid line), $t_3 = 0.90$ (dashed line).

We investigate how the transmission factor t, the coupling factors r_2 and r_3 influence the transmission spectrum (figure 2). The smaller the coupling factor r_2 and transmission factor t, and bigger the coupling factor r_3, the better will be EIT-like transmission spectrum.

2.2 *Circularly distributed*

If we take $\xi = \eta = \varsigma = 1$, we have $q = 2$, $\xi = 1 - 3\varepsilon/\sqrt{2}$, $\eta = 1 + 3\varepsilon/\sqrt{2}$. Substituting these into eq. (3), the eigenvalues are $x_1 = 1$, $x_2 = -1/2$, $x_3 = -1/2$, which are two-fold degenerate. They are the same as eq. (25) in ref. [9]. In this paper, we shall take $\xi = 1 - 3\varepsilon/\sqrt{2}$, $\eta = 1 + 3\varepsilon/\sqrt{2}$, $\varsigma = 1$, we have $p = -3$, $q = 2 - (3\varepsilon)^2$, $n = 2$, where ε is a non-degenerate factor. Substituting it into eq. (3), the eigenvalues are

$$x_1 = -(1 - \sqrt{3}\varepsilon)/2, \quad x_2 = -(-2 + \varepsilon^2)/2, \quad x_3 = -(1 + \sqrt{3}\varepsilon)/2. \tag{13}$$

When $\varepsilon \to 0$, the matrix element $\alpha_1 = \alpha_2 = \alpha_3 = \mathrm{e}^{jx_1\tau} + \mathrm{e}^{jx_2\tau}/2 = \gamma_1$, $\delta = \mu = \kappa = \rho = \nu = \zeta = (-\mathrm{e}^{jx_1\tau} + \mathrm{e}^{jx_2\tau})/3 = \gamma_2$, and the transfer matrix becomes

$$R(\tau) = \begin{pmatrix} \gamma_1 & \gamma_2 & \gamma_2 \\ \gamma_2 & \gamma_1 & \gamma_2 \\ \gamma_2 & \gamma_2 & \gamma_1 \end{pmatrix},$$

and this is eq. (29) in ref. [9]. An application of 3 × 3 circularly directional coupler in a wavelength-division, de-multiplexer based on a 2 × 3 or 3 × 3 Mach–Zehnder interferometer [9].

When $\varepsilon \neq 0$, the transfer matrix is

$$R(\tau) = \begin{pmatrix} \dfrac{\mathrm{e}^{jx_1\tau}}{N_1} & \dfrac{\mathrm{e}^{jx_2\tau}}{\sqrt{3}} & -\dfrac{\mathrm{e}^{jx_3\tau}}{N_2} \\ \dfrac{(-\sqrt{6}+1)\mathrm{e}^{jx_1\tau}}{N_1} & \dfrac{\mathrm{e}^{jx_2\tau}}{\sqrt{3}} & -\dfrac{(\sqrt{6}+1)\mathrm{e}^{jx_3\tau}}{N_2} \\ \dfrac{(-2+\sqrt{6})\mathrm{e}^{jx_1\tau}}{N_1} & \dfrac{\mathrm{e}^{jx_2\tau}}{\sqrt{3}} & \dfrac{(2+\sqrt{6})\mathrm{e}^{jx_3\tau}}{N_2} \end{pmatrix}$$

$$\times \begin{pmatrix} \dfrac{N_1(3+2\sqrt{6})}{6\sqrt{6}} & -\dfrac{N_1(3+\sqrt{6})}{6\sqrt{6}} & -\dfrac{N_1}{6} \\ 1/\sqrt{3} & 1/\sqrt{3} & 1/\sqrt{3} \\ \dfrac{N_2(3-2\sqrt{6})}{6\sqrt{6}} & -\dfrac{N_2(3-\sqrt{6})}{6\sqrt{6}} & \dfrac{N_2}{6} \end{pmatrix},$$

where

$$N_1 = \sqrt{6}\sqrt{3-\sqrt{6}}, \quad N_2 = \sqrt{6}\sqrt{3+\sqrt{6}}. \tag{14}$$

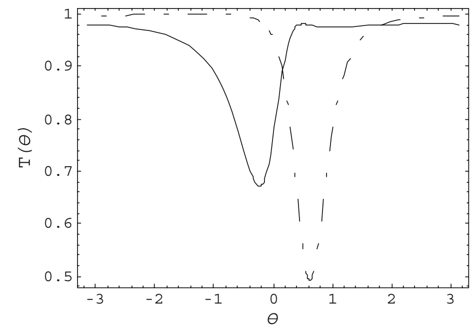

Figure 3. The transmission spectrum of the coupled double-ring resonator for frequencies θ (in GHz) with $r_2 = 0.85$, $r_3 = 0.99$, $t = 0.80$, $\varepsilon = 0$ (solid line), $\varepsilon = 1$ (the dashed line).

The transmission

$$T = \left|\alpha_1 + \frac{\kappa\delta B_1 + \rho\mu B_3 + [\delta(\rho^2 - \kappa\alpha_3) + \mu(\kappa\mu - \alpha_1\rho)]B_1 B_3}{1 - \alpha_1 B_1 - \alpha_3 B_3 + (\alpha_1\alpha_3 - \rho\mu)B_1 B_3}\right|^2. \quad (15)$$

We take the same parameters as in figure 2 and the transmission spectrum is shown in figure 3.

We find that the coupling factors r_2 and r_3, and the transmission factor t have nothing to do with the shape of transmission spectrum. The transmission spectrum remains Lorentz profile. We can see that the non-degenerate factor ε significantly influences transmission profile as shown in figure 3.

3. The 4 × 4 linearly distributed coupler

As shown in figure 4, a_1, b_1 is waveguide 1. When the light circuits in clockwise direction in microring 1 ($b_4 \to a_4 \to b_4$), we have $a_4 = B_4 b_4 = r_3 e^{j\theta} b_4$. When the light circuits in counterclockwise direction in microring 2 ($b_2 \to a_2 \to a_3 \to b_3 \to b_2$), we have $a_2 = \tau_1 r_2 e^{-j\theta} b_2 = \tau_1 B_2 b_2$ and $a_3 = \tau_1 b_3$, where τ_1 is the transmission through ring 1.

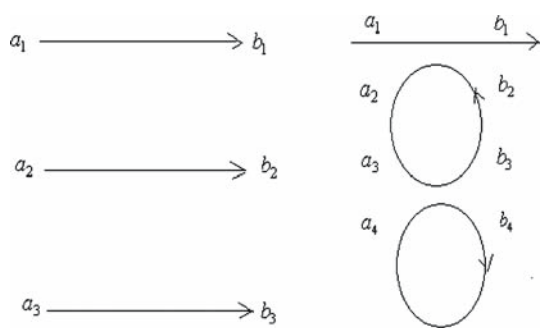

Figure 4. Schematic diagram of the 4 × 4 asymmetric coupler.

Without loss of generality, considering mode coupling between non-adjacent waveguides, the coupled-mode equation of linearly distributed 4×4 asymmetric coupler can be described by [9]

$$\begin{pmatrix} \dfrac{\partial a_1}{\partial z} \\ \dfrac{\partial a_2}{\partial z} \\ \dfrac{\partial a_3}{\partial z} \\ \dfrac{\partial a_4}{\partial z} \end{pmatrix} = \begin{pmatrix} 0 & j\,(K/2)\,\xi & 0 & 0 \\ j\,(K/2)\,\xi & 0 & j\,(K/2)\,\eta & 0 \\ 0 & j\,(K/2)\,\eta & 0 & j\,(K/2)\,\varsigma \\ 0 & 0 & j\,(K/2)\,\varsigma & 0 \end{pmatrix} \begin{pmatrix} a_1 \\ a_2 \\ a_3 \\ a_4 \end{pmatrix}. \tag{16}$$

The eigenfunction eq. (16) is

$$\begin{vmatrix} \lambda & j(K/2)\xi & 0 & 0 \\ j(K/2)\,\xi & \lambda & j(K/2)\eta & 0 \\ 0 & j(K/2)\eta & \lambda & j(K/2)\varsigma \\ 0 & 0 & j(K/2)\varsigma & \lambda \end{vmatrix} = \lambda^4 + \frac{K^2}{4}(\xi^2+\eta^2+\varsigma^2)\lambda^2 + \frac{K^4}{16}\xi^2\varsigma^2 = 0. \tag{17}$$

Setting $\lambda_i = jKx_i$, $i = 1$–4, $p = -(\xi^2 + \eta^2 + \varsigma^2)$, the eigenvalues x_i are

$$2x_1 = \sqrt{-\frac{p}{2} + \sqrt{\left(-\frac{p}{2}\right)^2 - \xi^2\varsigma^2}} = -2x_2,$$

$$2x_3 = \sqrt{-\frac{p}{2} - \sqrt{\left(-\frac{p}{2}\right)^2 - \xi^2\varsigma^2}} = -2x_4. \tag{18}$$

The corresponding eigenvector $\varphi_i(x_i)$ are

$$\begin{aligned}
&\varphi_1(x_1) = \varphi_1(x_2) = N_1\xi, \quad \varphi_2(x_1) = -\varphi_2(x_2) = N_1(2x_1), \\
&\varphi_3(x_3) = -\varphi_3(x_4) = N_3(2x_3), \quad \varphi_4(x_3) = \varphi_4(x_4) = N_3\varsigma \\
&\varphi_3(x_1) = \varphi_3(x_2) = \frac{N_1\eta(2x_1)^2}{(2x_1)^2 - \varsigma^2}, \quad \varphi_2(x_3) = \varphi_2(x_4) = \frac{N_3\eta(2x_3)^2}{(2x_3)^2 - \xi^2}, \\
&\varphi_4(x_1) = -\varphi_4(x_2) = \frac{N_1\eta\varsigma(2x_1)}{(2x_1)^2 - \varsigma^2}, \\
&\varphi_1(x_3) = -\varphi_1(x_4) = \frac{N_3\eta\xi(2x_3)}{(2x_3)^2 - \xi^2}.
\end{aligned} \tag{19}$$

In terms of $\sum_{i=1}^{4}\varphi_i^2(x_1) = 1$, $\sum_{i=1}^{4}\varphi_i^2(x_3) = 1$, we can deduce N_1 and N_3, respectively.

To construct a solution matrix

$$\chi(\tau) = \begin{pmatrix} \varphi_1(x_1)e^{jx_1\tau} & \varphi_1(x_2)e^{-jx_1\tau} & \varphi_1(x_3)e^{jx_3\tau} & \varphi_1(x_4)e^{-jx_3\tau} \\ \varphi_2(x_1)e^{jx_1\tau} & \varphi_2(x_2)e^{-jx_1\tau} & \varphi_2(x_3)e^{jx_3\tau} & \varphi_2(x_4)e^{-jx_3\tau} \\ \varphi_3(x_1)e^{jx_1\tau} & \varphi_3(x_2)e^{-jx_1\tau} & \varphi_3(x_3)e^{jx_3\tau} & \varphi_3(x_4)e^{-jx_3\tau} \\ \varphi_4(x_1)e^{jx_1\tau} & \varphi_4(x_2)e^{-jx_1\tau} & \varphi_4(x_3)e^{jx_3\tau} & \varphi_4(x_4)e^{-jx_3\tau} \end{pmatrix}. \tag{20}$$

When $\tau \to 0$, the inverse of eq. (20) is

$$\chi^{-1}(0) = \begin{pmatrix} \tilde{\phi}_1(x_1) & \tilde{\phi}_2(x_1) & \tilde{\phi}_3(x_1) & \tilde{\phi}_4(x_1) \\ \tilde{\phi}_1(x_2) & \tilde{\phi}_2(x_2) & \tilde{\phi}_3(x_2) & \tilde{\phi}_4(x_2) \\ \tilde{\phi}_1(x_3) & \tilde{\phi}_2(x_3) & \tilde{\phi}_3(x_3) & \tilde{\phi}_4(x_3) \\ \tilde{\phi}_1(x_4) & \tilde{\phi}_2(x_4) & \tilde{\phi}_3(x_4) & \tilde{\phi}_4(x_4) \end{pmatrix}. \tag{21}$$

When $\varsigma \to 0$, $x_1 = 1/\sqrt{2} = -x_2$, $x_3 = x_4 = 0$, the 4×4 linearly directional coupler is composed of one 3×3 linearly directional coupler and one fibre waveguide [10].

$$R(\tau)=\begin{pmatrix} (\xi^2/2)\cos[\tau/\sqrt{2}]+\eta^2/2 & j(\xi/\sqrt{2})\sin[\tau/\sqrt{2}] & (\xi\eta/2)\cos[\tau/\sqrt{2}]-(\xi\eta/2) & 0 \\ j(\xi/\sqrt{2})\sin[\tau/\sqrt{2}] & \cos[\tau/\sqrt{2}] & j(\eta/\sqrt{2})\sin[\tau/\sqrt{2}] & 0 \\ (\xi\eta/2)\cos[\tau/\sqrt{2}]-(\xi\eta/2) & j(\eta/\sqrt{2})\sin[\tau/\sqrt{2}] & (\xi^2/2)\cos[\tau/\sqrt{2}]+\eta^2/2 & 0 \\ 0 & 0 & 0 & 1 \end{pmatrix}. \tag{22}$$

When $\eta \to 0$, the 4×4 linearly directional coupler consists of two 2×2 linearly directional couplers.

$$R(\tau) = \begin{pmatrix} \cos[x_1\tau] & j\sin[x_1\tau] & 0 & 0 \\ j\sin[x_1\tau] & \cos[x_1\tau] & 0 & 0 \\ 0 & 0 & \cos[x_3\tau] & j\sin[x_3\tau] \\ 0 & 0 & j\sin[x_3\tau] & \cos[x_3\tau] \end{pmatrix}. \tag{23}$$

When $\eta \neq 0$, the transfer matrix is

$$R(\tau) = \chi(\tau)\chi^{-1}(0) = \begin{pmatrix} \alpha_1 & \delta & \mu & \kappa \\ \delta & \alpha_2 & \rho & \nu \\ \mu & \rho & \alpha_3 & \zeta \\ \kappa & \nu & \zeta & \alpha_4 \end{pmatrix}$$

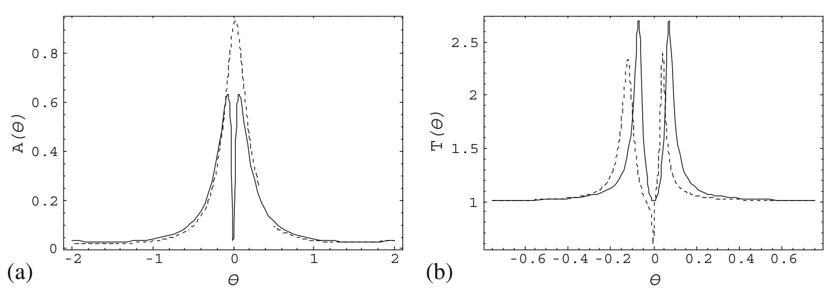

Figure 5. Absorption and transmission spectra of the coupled double-ring resonator for frequencies θ (in GHz) with $\xi = 1$, $\varsigma = 0.001$, $\eta = 0$ (solid line), $\eta = 0.5$ (dashed line), $r_3 = 0.9999$, $t_2 = 0.995$. (**a**) $r_2 = 0.88$, $t_3 = r_2 r_3 = 0.879912$, (**b**) $r_2 = 1.07$, $t_3 = 0.94$.

where

$$
\begin{aligned}
\alpha_1 &= \varphi_1^2(x_1)\,\mathrm{e}^{jx_1\tau} + \varphi_1^2(x_2)\mathrm{e}^{-jx_1\tau} + \varphi_1^2(x_3)\,\mathrm{e}^{jx_3\tau} + \varphi_1^2(x_4)\,\mathrm{e}^{-jx_3\tau},\\
\alpha_2 &= \varphi_2^2(x_1)\,\mathrm{e}^{jx_1\tau} + \varphi_2^2(x_2)\mathrm{e}^{-jx_1\tau} + \varphi_2^2(x_3)\,\mathrm{e}^{jx_3\tau} + \varphi_2^2(x_4)\,\mathrm{e}^{-jx_3\tau},\\
\alpha_3 &= \varphi_3^2(x_1)\,\mathrm{e}^{jx_1\tau} + \varphi_3^2(x_2)\mathrm{e}^{-jx_1\tau} + \varphi_3^2(x_3)\,\mathrm{e}^{jx_3\tau} + \varphi_3^2(x_4)\,\mathrm{e}^{-jx_3\tau},\\
\alpha_4 &= \varphi_4^2(x_1)\,\mathrm{e}^{jx_1\tau} + \varphi_4^2(x_2)\mathrm{e}^{-jx_1\tau} + \varphi_4^2(x_3)\,\mathrm{e}^{jx_3\tau} + \varphi_4^2(x_4)\,\mathrm{e}^{-jx_3\tau},\\
\delta &= \varphi_1(x_1)\varphi_2(x_1)\,\mathrm{e}^{jx_1\tau} + \varphi_1(x_2)\varphi_2(x_2)\,\mathrm{e}^{-jx_1\tau} + \varphi_1(x_3)\varphi_2(x_3)\mathrm{e}^{jx_3\tau}\\
&\quad + \varphi_1(x_4)\varphi_2(x_4)\mathrm{e}^{-jx_3\tau},\\
\mu &= \varphi_1(x_1)\varphi_3(x_1)\,\mathrm{e}^{jx_1\tau} + \varphi_1(x_2)\varphi_3(x_2)\mathrm{e}^{-jx_1\tau} + \varphi_1(x_3)\varphi_3(x_3)\mathrm{e}^{jx_3\tau}\\
&\quad + \varphi_1(x_4)\varphi_3(x_4)\mathrm{e}^{-jx_3\tau},\\
\kappa &= \varphi_1(x_1)\varphi_4(x_1)\,\mathrm{e}^{jx_1\tau} + \varphi_1(x_2)\varphi_4(x_2)\mathrm{e}^{-jx_1\tau} + \varphi_1(x_3)\varphi_4(x_3)\mathrm{e}^{jx_3\tau}\\
&\quad + \varphi_1(x_4)\varphi_4(x_4)\mathrm{e}^{-jx_3\tau},\\
\rho &= \varphi_2(x_1)\varphi_3(x_1)\,\mathrm{e}^{jx_1\tau} + \varphi_2(x_2)\varphi_3(x_2)\mathrm{e}^{-jx_1\tau} + \varphi_2(x_3)\varphi_3(x_3)\mathrm{e}^{jx_3\tau}\\
&\quad + \varphi_2(x_4)\varphi_3(x_4)\mathrm{e}^{-jx_3\tau},\\
\nu &= \varphi_2(x_1)\varphi_4(x_1)\,\mathrm{e}^{jx_1\tau} + \varphi_2(x_2)\varphi_4(x_2)\mathrm{e}^{-jx_1\tau} + \varphi_2(x_3)\varphi_4(x_3)\mathrm{e}^{jx_3\tau}\\
&\quad + \varphi_2(x_4)\varphi_4(x_4)\mathrm{e}^{-jx_3\tau},\\
\zeta &= \varphi_3(x_1)\varphi_4(x_1)\,\mathrm{e}^{jx_1\tau} + \varphi_3(x_2)\varphi_4(x_2)\mathrm{e}^{-jx_1\tau} + \varphi_3(x_3)\varphi_4(x_3)\mathrm{e}^{jx_3\tau}\\
&\quad + \varphi_3(x_4)\varphi_4(x_4)\mathrm{e}^{-jx_3\tau}.
\end{aligned}
\tag{24}
$$

We can describe the interaction by the matrix relation

$$
\begin{pmatrix} b_1\\ b_2\\ b_3\\ b_4 \end{pmatrix} = \begin{pmatrix} \alpha_1 & \delta & \mu & \kappa\\ \delta & \alpha_2 & \rho & \nu\\ \mu & \rho & \alpha_3 & \zeta\\ \kappa & \nu & \zeta & \alpha_4 \end{pmatrix} \begin{pmatrix} a_1\\ B_2 b_2 \tau_1\\ b_3\tau_1\\ B_4 b_4 \end{pmatrix}. \tag{25}
$$

The transmission

$$
T(\theta) = \left| \alpha_1 + (\delta B_2 + \mu B_3)\tau_1 \frac{b_2}{a_1} + \kappa B_4 \frac{b_4}{a_1} \right|^2,
$$

where

$$
\frac{b_2}{a_1} = \frac{\delta(1-\alpha_4 B_4) + \kappa\nu B_4}{(1-\alpha_2 B_2\tau_1 - \rho B_3\tau_1)(1-\alpha_4 B_4) - \nu B_4(\nu B_2 + \zeta B_3)\tau_1},
$$

$$
\frac{b_4}{a_1} = \frac{\kappa(1-\alpha_2 B_2\tau_1 - \rho B_3\tau_1) + \delta(\nu B_2 + \zeta B_3)\tau_1}{(1-\alpha_2 B_2\tau_1 - \rho B_3\tau_1)(1-\alpha_4 B_4) - \nu B_4(\nu B_2 + \zeta B_3)\tau_1}. \tag{26}
$$

The transmission of the first ring $\tau_1 = (t_1 - B_4)/(1 - t_1 B_4)$ has nothing to do with parameters of the second ring [1] (figure 5).

By increasing the value of η, the absorption spectrum changes from a typical all-optical EIT-like profile to Lorentz profile. The peak value of absorption spectrum increases. The transmission spectrum remains EIT-like, the peak value of transmission spectrum declines. For $\eta = 0$, the solid curve is in agreement with figure 2 and figure 4 in ref. [6], respectively.

Acknowledgements

This work was supported by the State Key Laboratory of Quantum Optics and Quantum Optics Devices, Shanxi University, Shanxi, China (Grant No. KF201401) and the National Natural Science Foundation of China (Grant No. 11504074).

Appendix A

Comparing

$$\begin{pmatrix} x & \xi & \varsigma \\ \xi & x & \eta \\ \varsigma & \eta & x \end{pmatrix} \begin{pmatrix} \varphi_1 \\ \varphi_2 \\ \varphi_3 \end{pmatrix} = 0$$

with

$$\begin{pmatrix} a_{11} & a_{12} & a_{13} \\ a_{21} & a_{22} & a_{23} \\ a_{31} & a_{32} & a_{33} \end{pmatrix} \begin{pmatrix} A_{11} \\ A_{21} \\ A_{31} \end{pmatrix} = 0,$$

we have

$$\begin{pmatrix} x & \xi & \varsigma \\ \xi & x & \eta \\ \varsigma & \eta & x \end{pmatrix} = \begin{pmatrix} a_{11} & a_{12} & a_{13} \\ a_{21} & a_{22} & a_{23} \\ a_{31} & a_{32} & a_{33} \end{pmatrix}, \quad \varphi_1 = A_{11}, \quad \varphi_2 = A_{21}, \quad \varphi_3 = A_{31}. \tag{A.1}$$

and

$$\begin{vmatrix} a_{11} & a_{12} & a_{13} \\ a_{21} & a_{22} & a_{23} \\ a_{31} & a_{32} & a_{33} \end{vmatrix} = a_{11}A_{11} + a_{12}A_{21} + a_{13}A_{31},$$

where

$$A_{11} = \begin{vmatrix} a_{22} & a_{23} \\ a_{32} & a_{33} \end{vmatrix}, \quad A_{21} = -\begin{vmatrix} a_{21} & a_{23} \\ a_{31} & a_{33} \end{vmatrix}, \quad A_{31} = \begin{vmatrix} a_{21} & a_{22} \\ a_{31} & a_{32} \end{vmatrix}. \tag{A.2}$$

References

[1] D D Smith, H Chang, K A Fuller, A T Rosenberger and R W Boyd, *Phys. Rev. A* **69**, 063804 (2004)
[2] M Fleischhauer, A Imamoglu and J P Marangos, *Rev. Mod. Phys.* **77**, 633 (2005)
[3] K Totsuka, N Kobayashi and M Tomita, *Phys. Rev. Lett.* **98**, 213904 (2007)
[4] J K Poon, L Zhu, G A DeRose and A Yariv, *Opt. Lett.* **31**, 456 (2006)
[5] D D Smith and H Chang, *J. Mod. Opt.* **51**, 2503 (2004)
[6] X Liu, M Kong and H Feng, *J. Opt. Soc. Am. B* **29**, 68 (2012)
[7] C Zheng, X Jiang, S Hua, L Chang, G Li, H Fan and M Xiao, *Opt. Exp.* **20**, 18319 (2012)
[8] Y F Xiao, X F Jiang, Q F Yang, L Wang, K B Shi, Y Li and Q H Gong, *Laser Photon. Rev.* **7**, L51 (2013)
[9] Y C Meng, Q Z Guo, W H Tan and Z M Huang, *J. Opt. Soc. Am. A* **21**, 1518 (2004)
[10] C Y Zhao and W H Tan, *J. Mod. Opt.* **62**, 313 (2015)